Kashif *et al. Chem. Biol. Technol. Agric.* (2023) 10:145
https://doi.org/10.1186/s40538-023-00513-5

Chemical and Biological Technologies in Agriculture

RESEARCH

Open Access

Microbial degradation of pyridine: a proposed nitrogen metabolism pathway deciphered in marine mangrove *Bacillus aryabhattai* strain NM1-A2

Muhammad Kashif[1,5†], Lirong Bai[4†], Jianwen Xiong[3], Shuming Mo[1,5], Yimeng Sang[5], Kunmei Huang[5], Jingjing Song[4], Syed Jalil Shah[6], Sohail Khan[7], Taj Malook Khan[8] and Chengjian Jiang[1,2,5*]

Abstract

Background Diverse microbes, such as bacteria, are of immense worth to mangrove ecosystems due to their adaptability to salinity and variable environmental characteristics conditions. Pyridine and its derivatives compose most heterocyclic aromatic compounds largely produced by human activities that lead to environmental pollution. Bacteria have a crucial role in the nutrient cycling of carbon and nitrogen etc., to understand their functional involvement with environmental factors or ecosystem functioning as well as the species invasion and domestic or agriculture pyridine degradation pollution activities that threaten the mangrove ecosystem.

Methods This work established the genetic-based molecular degradation of organic compounds in the mangrove ecosystem, which ultimately makes the availability of nutrients. As well as the effects of various abiotic factors on pyridine degradation to discover the pyridine degradation and the removal of ammonia nitrogen and the proposed nitrogen metabolism pathway.

Results The novel bacterial strain NM1-A2 was isolated from mangrove sediments and, after 16S rRNA gene sequence analysis identified as *Bacillus aryabhattai*. NM1-A2 completely degraded pyridine within a 100 h incubation period at a temperature of 35 °C, an initial pH of 7.0, glucose and a pyridine concentration of 500 mg/L. The pseudo-first-order kinetics model described the pyridine biodegradation profile of NM1-A2 well. Interestingly, within 96 h the strain achieved almost complete pyridine degradation with a total organic carbon (TOC) removal of 87.9% ± 0.19% (from 377.52 ± 6.9 mg/L to 45.65 ± 0.14 mg/L). Within 96 h, the pyridine ring in the total nitrogen (TN) fraction at the maximum concentration of 55.31 ± 0.17 mg/L, furtherly 51.3% ± 2.39% of (TN) converted into Ammonia nitrogen (NH_4^+-N). Furthermore, NM1-A2 exhibited its pyridine biodegradation activity decreased by only 4% after three consecutive cycles (48 h each). Moreover, NM1-A2 possessed *nrt-ABCD* nitrate transport family and *gltABCD* operons that participate in the activities of glutamine and glutamate synthetase in NH_4^+ conversion in the nitrogen cycle. Furthermore, the nitrogen metabolism genes (*nrtA*, *nrtB*, *nrtC*, *nirB*, *nirD*, *gltB*, *gltD*, *glnA*) exhibited expression in NM1-A2.

Conclusion This research offers a potential treatment strategy for pyridine degradation in the mangrove ecosystem.

Keywords *Bacillus aryabhattai*, Pyridine degradation, Nitrogen metabolism, Mangrove environment

†Muhammad Kashif and Lirong Bai contributed equally to this work.

*Correspondence:
Chengjian Jiang
jiangcj0520@vip.163.com
Full list of author information is available at the end of the article

Graphical Abstract

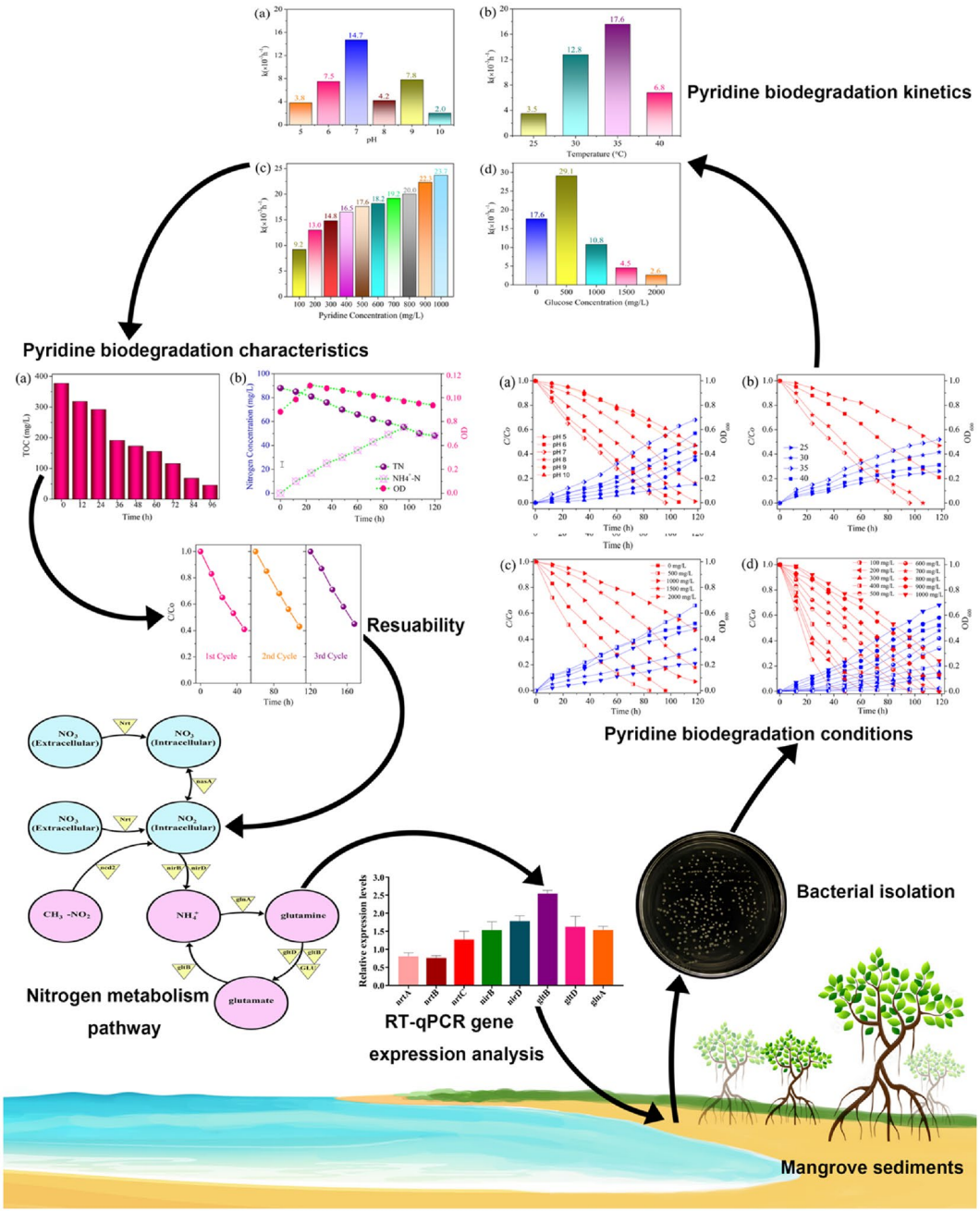

Background

Pyridine and its derivatives can be derived from coal or synthesized artificially and are commonly used as industrial solvents that inadvertently enter the environment. The global annual production of pyridine exceeds approximately 20,000 tons, and pyridine is frequently found in wastewater from the pharmaceutical industry and other related industries [1]. The average concentration of pyridine in wastewater released by industries producing pyridine and its metabolites is approximately 20–300 mg/L and may reach 600–1000 mg/L during emergency discharge [2, 3]. Pyridine-containing waste is highly toxic and emits a nauseating odor when discharged, Once released into aquatic ecosystems, such as water bodies, wastewater, and sewage, this pyridine-laden discharge, along with its derivatives, will endure in the aquatic environment for an extended duration. This persistence is anticipated to result in significant repercussions on both human health and environmental well-being [4]. Bioremediation is a viable solution for addressing ecological pollution caused by substituent chemicals, particularly pyridine and its derivatives [5]. Researchers have long shown interest in removing pyridine from the environment or wastewater [6, 7]. Hazardous pyridine and its derivatives can persist for prolonged periods in aquatic environments, posing risks to both human health and the environment [8].

The United States Environmental Protection Agency (EPA) has categorized pyridine as a primary concern among organic pollutants. According to the latest report from NBC, the global pyridine market is projected to reach an estimated value of USD 747.89 million by 2023 [9]. Current technologies enable pyridine treatment via coagulation, adsorption, Fenton oxidation, photocatalytic oxidation, chemical oxidation, and direct incineration techniques [10]. Biological treatments are preferred because they are more cost-effective and environmentally friendly than physical and chemical methods [11]. Microbes exhibit diverse phenotypes and possess distinct metabolic pathways that can degrade pyridines and their derivatives [12].

Mangrove tidal waters contain low concentrations of dissolved organic nitrogen (DON) and inorganic nitrogen in their molecular forms, which are accompanied by NH_4^+ and NO_3^- and NO_2^- [13, 14]. The DON in sediments is mostly refractory and consists primarily of humic substances, aromatic compounds, growth factors, and amino acids, among other constituents [15]. Ammonia–nitrogen is an essential Nitrogen (N) form in aquatic environments that plants, heterotrophic bacteria, and nitrifying bacteria can utilize. Ammonia–nitrogen is typically obtained from fertilizers such as urea, ammonia phosphate, and ammonia nitrate, diffusion from soil and aquaculture discharges [14]. Biodegradation is a highly appealing approach for the degradation of pyridine due to its ability to transform the chemical into relatively harmless byproducts, CO_2 and NH_4^+ etc., [16].

In mangrove soils, elevated salinity levels impede the production and functioning of nitrogen assimilation enzymes like nitrate reductase (NR), nitrite reductase (NiR), glutamate synthetase (GS), and glutamate synthase (GOGAT) [17], as well as the ability of plants to reduce and assimilate nitrogen [18]. Salinity-induced osmotic changes and reduced NO_3^- uptake may also inhibit the activity of nitrogen assimilation enzymes [19].

The isolation of pyridine-degrading microorganisms is the primary focus of previous research on the bioremediation of pyridine-contaminated environments. Such microorganisms include *Bacillus* [20], *Pseudonocardia* [21], *Nocardides* [22], *Pseudomonas* [23], *Paracoccus* [24], *Arthrobacter* [25], *Alcaligenes* [26], *Streptomyces* [27], *Rhodococcus* [12], *Shewanella* [28], and *Shinella* [8]. While a bioaugmentation approach, which involves enhancing the introduction of specific species into biological systems like activated sludge tanks, has been established for treating pyridine-contaminated wastewater, it is important for experts to shift their focus towards the development of a practical bioaugmentation approach that emphasizes pyridine biodegradation.

This study, comprehensively investigated pyridine biodegradation by *Bacillus aryabhattai* strain NM1-A2. In this research, the effects of various abiotic factors on pyridine biodegradation were investigated. The investigation of pyridine degradation intermediates, characteristics and the production of ammonia nitrogen by pyridine. Furthermore, we proposed a nitrogen metabolism pathway and gene expression associated with NM1-A2. The findings of our study showed that NM1-A2 could biodegrade pyridine, which could be employed for removing toxic ammonia products and has vast biotechnological and ecological prospects.

Materials and method

Sample collection

Sediment samples were collected from the subtropical mangrove wetlands in Beibu Gulf, South China Sea (21°29′25.74″N, 109°45′49.43″E) Additional file 1: Fig. S1; the detailed information is listed in our previous study [29].

Chemicals and growth medium

A pyridine standard sample was purchased from Sigma Aldrich, USA. Yeast extract and tryptone were obtained from Oxoid Ltd., U.K. All the other chemicals used in this study were of analytical grade. Their details are

provided in the supplementary material (Additional file 1: Table S1).

Mineral salt medium (MSM) and Luria Burtani media were used in this study. The detailed compositions of these media are given in the supplementary material (Additional file 1: Table S1) [29].

The strain's ability to degrade pyridine and the strain was cultured in liquid MSM (Additional file 1: Table S1) [30], and addition of (1 mL) trace element solution in MSM medium [31]. The composition of the growth medium is presented in the supplementary material (Additional file 1: Table S1). The phosphate buffers KH_2PO_4 and $Na_2HPO_4{\cdot}12H_2O$ were used to maintain MSM at a constant pH. Pyridine was added as the final sole carbon and nitrogen source. All media were autoclaved for 121 °C and 30 min [32].

Effect of pyridine biodegradation conditions

A pyridine biodegradation assay used 100 mL of MSM containing (100 µL) inocula with the optimal initial pyridine concentration of 500 mg/L. The initial pH of the reactors was set to 7.0 by varying the proportion of KH_2PO_4 and $Na_2HPO_4{\cdot}12H_2O$ in the buffer system at the optimal incubation temperature of 35 °C. Similarly, the effects of glucose concentrations of 0–2000 mg/L, initial pyridine concentrations of 100–2000 mg/L, pH levels of 5–10, and different temperatures of 25 °C–40 °C on pyridine degradation were evaluated while keeping other optimal conditions the same. The control test was also performed in the medium. All tests were conducted in triplicate, and the analyzed data's average and standard deviation (SD) were obtained Pyridine concentration was measured at 254 nm [33].

Pyridine degradation kinetics

The rate of pyridine degradation by NM1-A2 was investigated by fitting reaction kinetics curves with the pseudo-first-order model, which is shown as Eq. 1: [34]

$$\ln\left(C/C_0\right) = kt, \tag{1}$$

In contrast, the degradation ratio over time serves as a measure of pyridine biodegradation activity, with C/Co representing the relative pyridine concentration (where C is the actual pyridine concentration at each time interval and Co is the initial pyridine concentration). The variable "t" signifies the reaction time in hours, and the apparent rate constant (k) quantifies the speed of the degradation reaction. Additionally, we extracted pseudo-first-order apparent rate constant values from the degradation ratio data to characterize the reaction rate [35, 36].

Pyridine biodegradation characteristics

A visible spectrophotometer was used to detect the bacterial density at OD_{600}. All samples were centrifuged at 10,000 rpm and filtered using a 0.22 µm syringe filter. Nessler's reagent spectrophotometry method at a wavelength of 420 nm was conducted to detect and measure the concentration of NH_4^+-N [37]. Total nitrogen (TN) was observed with ultraviolet spectrophotometry and alkaline oxidation persulfate. The total organic carbon concentration was assessed using an Analytikjena TOC analyzer (TOC-multi N/c), while the pyridine content was computed through UV spectrophotometry at a wavelength of 256 nm. The data is presented as means ± standard deviation (SD) [38].

Pyridine recycling performance

Pyridine biodegradation assays were performed on NM1-A2 using batch reactors (Erlenmeyer flasks: 250 mL). NM1-A2 cells were cultured in liquid LB medium at 180 rpm and 30 °C for 48 h, then collected via centrifugation at 600 rpm and 4 °C for 10 min, and washed thrice with sterilized MSM (100 mL). Finally, inocula were prepared by diluting the bacterial deposits with MSM until an optical density of 2.0 at OD_{600} was reached. The prepared inocula were placed in 100 mL of liquid MSM solution with an inoculum size of 5% (v/v) for further study [39, 40].

Nitrogen metabolism pathway

After obtaining the whole-genome data of NM1-A2, the nitrogen metabolism functional genes of NM1-A2 were annotated through the following method: 1. The BLAST comparison of predicted genes was performed with each functional database (blastp, e value $\leq 1e^{-5}$). 2. BLAST results were filtered. For the BLAST result of each sequence, the comparison result with the highest score was selected (default identity $\geq$ 40%, coverage $\geq$ 40%) for the annotation [41, 42].

RT-qPCR gene expression analysis

Total RNA was extracted from the bacterial strain NM1-A2 using the total RNA rapid extraction kit (Nanjing Yifeixue Biotechnology Co., Ltd, China) following the manufacturer's instructions. cDNA was synthesized using the cDNA first-strand rapid synthesis kit (Nanjing Yifeixue Biotechnology Co., Ltd, China). Specific pairs of primers for each gene were used for RT-qPCR analysis, and 200 ng of cDNA was used as the template. For RT-qPCR analysis, specific primer pairs were employed

for each gene, and 200 ng of cDNA served as the template. The RT-qPCR was carried out using the SYBR Green qPCR Master Mix on a Light Cycler 480 instrument (Roche Applied Science, Nonnenwald, Penzberg, Germany) with three replicates. The reaction mixture had a total volume of 20 µL, comprising 10 µL of SYBR Green, 2 µL of cDNA template, 0.4 µL of each forward and reverse primer, and 7.2 µL of PCR-grade water. The thermal cycling conditions were as follows: pre-incubation (95 °C for 5 min), amplification (95 °C for 10 s, 60 °C for 10 s, and 72 °C for 10 s, for 45 cycles), melting (95 °C for 30 s, 72 °C for 5 min), and cooling (40 °C for 30 s). The Actin gene was employed as an internal control for normalization. The resulting data were analyzed using the $2^{\wedge(-ct)}$ method [43]. The respective genes specific primers and sequences are presented in Additional file 1 (Table S2) and Additional file 2.

Results

Effect of pyridine biodegradation conditions

Complete pyridine biodegradation and maximum cell growth were achieved within 100 h at an initial pH of 7.0. However, as shown in Fig. 1a, pyridine biodegradation and cell growth were delayed under acidic or alkaline pH conditions. Cell growth and pyridine degradation at the incubation temperatures of 35 °C and 40 °C were vastly enhanced relative to those at 25 °C and 30 °C (Fig. 1b). As depicted in Fig. 1c, 500 mg/L optimum doses of pyridine could be degraded in the presence of 500 mg/L glucose concentration. Correspondingly, 500 mg/L glucose significantly enhanced cell growth. Although cell growth was significantly accelerated, pyridine elimination was significantly suppressed, particularly at high glucose doses, when the glucose concentration was increased from 500 to 2000 mg/L, reducing the degradation activity. As illustrated in Fig. 1d, biodegradation activity decreased as the initial 500 mg/L pyridine concentration from 100 mg/L to 1000 mg/L (Fig. 1).

Pyridine degradation kinetics

Effect of initial pH

NM1-A2 showed high pyridine biodegradation (1.47×10^{-2}/h) at pH 7 and under highly acidic conditions. A basic medium was unsuitable for the pyridine biodegradation activity of NM1-A2. Therefore, pH 7 was the optimal pH for pyridine biodegradation by NM1-A2 (Fig. 2a).

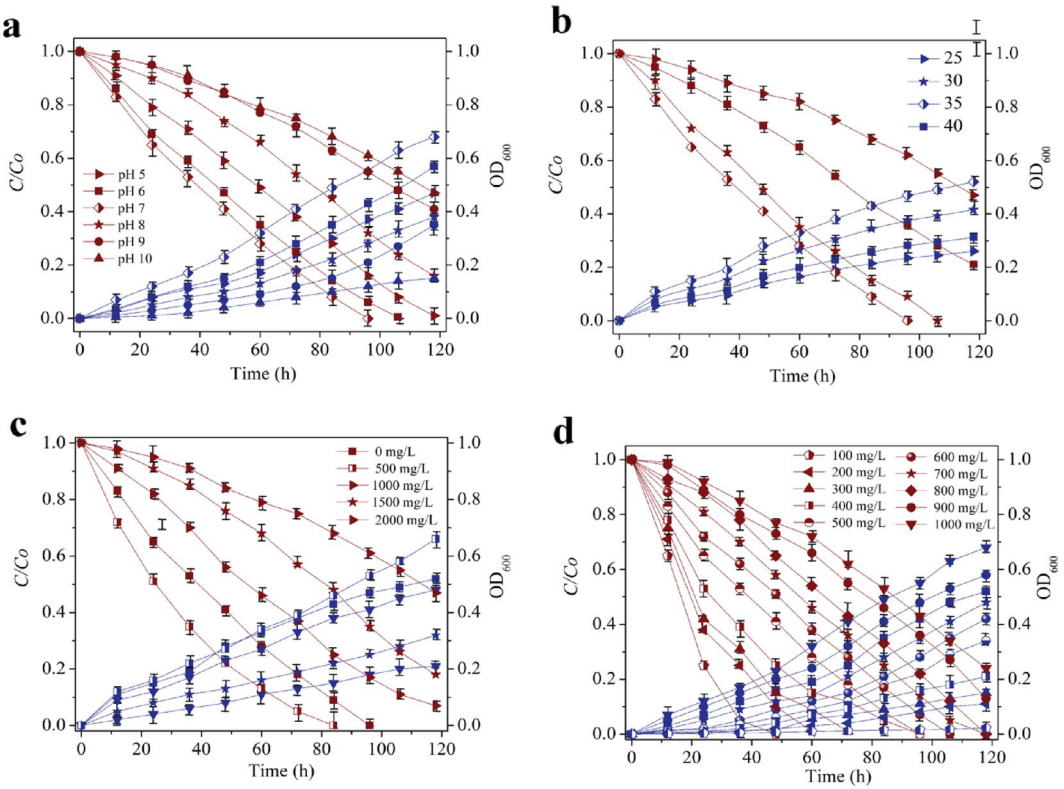

Fig. 1 **a** Effect of initial pH, **b** temperature, **c** glucose concentration, and **d** initial pyridine concentration on NM1-A2 cell growth and pyridine biodegradation

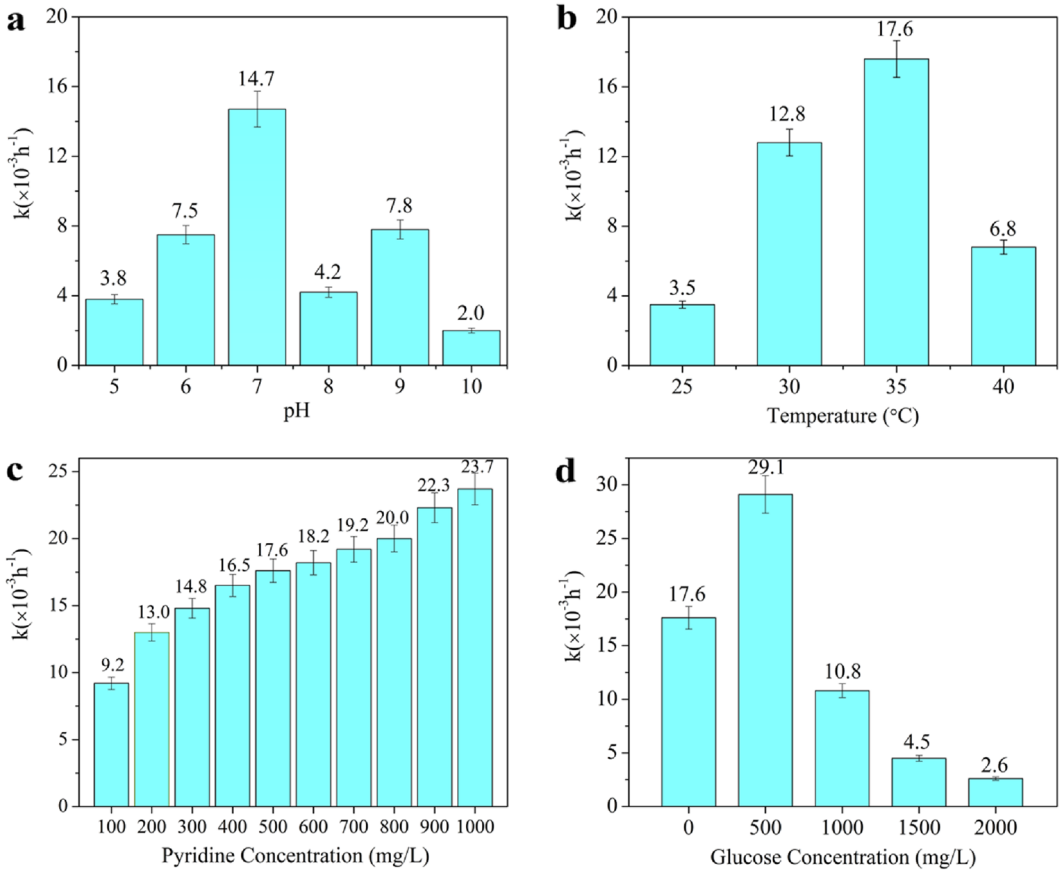

Fig. 2 Effect of **a** pH, **b** temperature, **c** initial pyridine concentration, and **d** glucose concentration on the pseudo-first-order apparent rate constants of pyridine biodegradation by NM1-A2

Effect of temperature

The optimal temperature for the growth of NM1-A2 was 35 °C, at which pyridine biodegradation (1.76×10^{-2}/h) was enhanced. Biodegradation activity regularly increased when the temperature was increased from 25 °C to 35 °C but decreased to 0.68×10^{-2}/h at temperatures beyond 35 °C (Fig. 2b).

Effect of pyridine concentration

The degradation activity decreased as the initial pyridine concentration was raised (from 0.92×10^{-2}/h to 2.37×10^{-2}/h). In high-concentration media, where pyridine levels increased from 100 to 1000 mg/L, more pyridine molecules competed, stimulating the bacterial strain to simultaneously degrade the higher quantity of molecules (Fig. 2c). The NM1-A2 was responsible for the high pyridine removal observed in a concentrated pyridine medium. The enhanced bacterial growth at a high pyridine concentration has high potential for commercial biodegradation. However, 500 mg/L was chosen as the optimal pyridine concentration because commercial oil contains less than 500 mg/L pyridine (Fig. 2c).

Effect of glucose concentration

Glucose contents of 0–2000 mg/L were used to evaluate the effect of glucose on the reaction kinetics of pyridine degradation by NM1-A2. Figure 2d shows that with the increase in glucose content from 0 mg/L to 500 mg/L, the pyridine degradation rate continuously increased from 1.76×10^{-2}/h to 2.91×10^{-2}/h. With the addition of 500 mg/L glucose concentration, the apparent rate constant gradually reduced to 0.26×10^{-2}/h. Consequently, high glucose content was responsible for the pyridine degradation by NM1-A2 (Fig. 2d).

Pyridine biodegradation characteristics

NM1-A2 was inoculated into MSM containing 500 mg/L pyridine. Figure 3a illustrates that after 25 h of the experiment, the strain entered the logarithmic phase with a maximum OD_{600} of 0.117 ± 0.028.

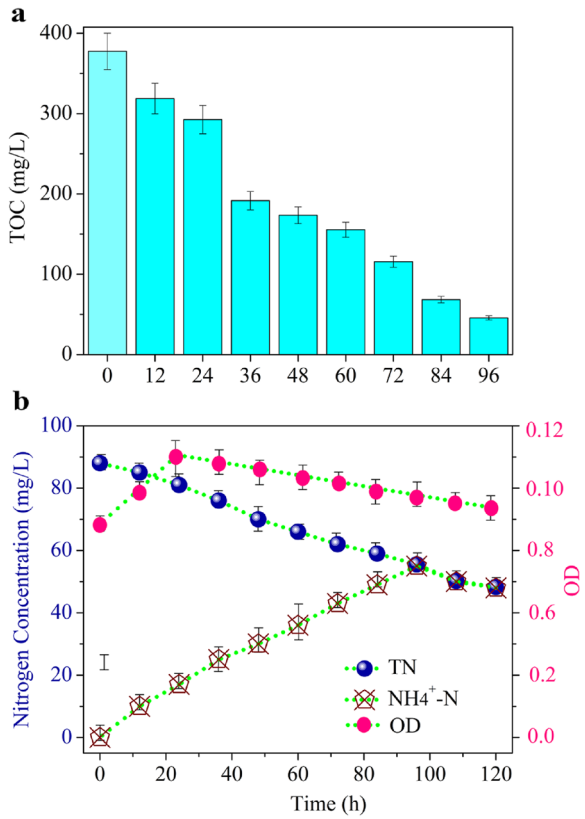

Fig. 3 Growth and degradation performance of NM1-A2 at an initial pyridine concentration of 500 mg/L. **a** Effect of TOC degradation. **b** Effect of TN and NH_4^+-N concentration

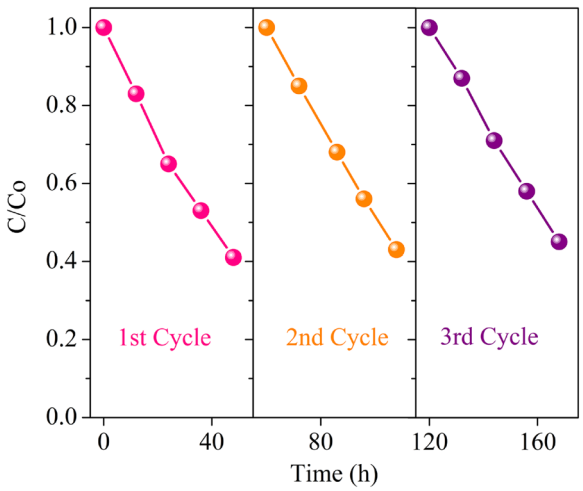

Fig. 4 Performance of NM1-A2 in different cycles of pyridine degradation

The strain could flourish solely with pyridine as a carbon and nitrogen source. Within 96 h, 500 mg/L pyridine was removed, and the TOC decreased from 377.52 ± 6.9 mg/L to 45.65 ± 0.14 mg/L, reflecting a removal efficiency of 87.9% ± 0.19%. A high TOC removal efficiency is indicative of a high capacity for pyridine mineralization. This result demonstrated that the isolated strain could oxidize pyridine and perform mineralization efficiently. During pyridine biodegradation, the nitrogen in the pyridine ring was transformed into NH_4^+-N. Strain expansion resulted in a considerable increase in NH_4^+-N, as shown in Fig. 3b. During 96 h of the experiment, TN was mainly converted into NH_4^+-N, which reached a maximum concentration of 55.31 ± 0.17 mg/L. A total of 51.3% ± 2.39% of TN was converted into NH_4^+-N. However, the strain could not further convert TN beyond this concentration (Fig. 3).

Recycling performance

Pyridine degradation was carried out for three consecutive cycles to investigate the recycling performance of the bacterial strain NM1-A2 and determine its practicability on an industrial scale. After 48 h of the first cycle, NM1-A2 was washed with fresh MSM for reuse for pyridine degradation. The same process was performed for the third cycle. Pyridine degradation declined by 4% after three consecutive cycles. This result proved that NM1-A2 could be reused multiple times for the degradation of pyridine, a refractory nitrogen compound. Therefore, NM1-A2 can be used as a practical bacterial strain for industrial-scale degradation in petroleum refineries. By contrast, many other bacteria cannot survive and be reused under harsh environmental conditions (Fig. 4).

Nitrogen metabolism pathway

Eleven directly homologous genes associated with nitrogen metabolism were identified through KEGG database annotation, and 20 nitrogen cycle genes were annotated in ncycdb by using diamond. The results of the two databases were comprehensively and comparatively analyzed to map the relevant nitrogen cycle.

The nitrogen metabolism analysis results of NM1-A2 showed that *nrt-ABCD* was annotated in NM1-A2. Nitrate and nitrite have been identified to possess a relatively similar transport mechanism involving the *nrt-ABCD* transport family and *gltABCD* operons. Within plants, salinity disrupts the capacity to reduce and incorporate nitrogen, primarily by diminishing the synthesis and functioning of nitrogen assimilation enzymes. NM1-A2 can generate NO_2 via the following reaction: ethylnitronate + oxygen + reduced FMN < = > acetaldehyde + nitrite + FMN + H_2O. In cells, NO_2 and NO_3 can be converted into each other by nitrite receptor oxidoreductase as nitrite + acceptor + H_2O < = > nitrate + reduced acceptor. *nirB* and *nirD* genes were also found in NM1-A2 cells. *nirB* and

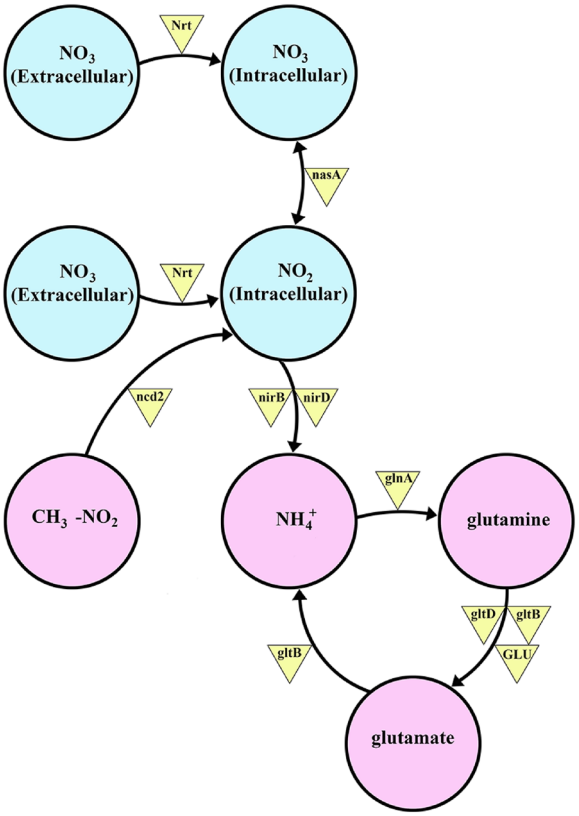

Fig. 5 Proposed nitrogen metabolism pathway by strain NM1-A2

nirD are essential for NADH-dependent NiR activity. In cells, nitrate or nitrite is transformed into ammonium for integration into carbon skeletons. Nitrate is first converted into nitrite by nitrate reductase (NR). Then, nitrite is converted into ammonium by NiR as ammonia + 3 NAD^+ + 2 H_2O < = > nitrite + 3 NADH + 3 H^+.

Moreover, the ammonium in NM1-A2 can generate glutamine through the action of amine ligase then glutamate through the catalytic reaction ATP + L-glutamate + ammonia < = > ADP + orthophosphate + L-glutamine for entry into amino acid metabolism and use as intracellular material. Therefore, NM1-A2 might be biodegraded pyridine. (Fig. 5).

RT-qPCR gene expression analysis

RT-qPCR was performed to verify the expression of genes related to nitrogen metabolism. The findings demonstrated that all nitrogen metabolism-associated genes (*nrtA*, *nrtB*, *nrtC*, *nirB*, *nirD*, *gltB*, *gltD*, *glnA*) exhibited expression in bacterial strain NM1-A2 (Fig. 6). The RT-qPCR products were verified by 1% agarose gel electrophoresis, and the bands were confirmed, as depicted in (Additional file 1: Fig. S2).

Discussion

Pyridine, a heterocyclic aromatic compound, holds importance in mangrove ecosystems due to both natural occurrences and human influence [44]. Excessive pyridine contamination can disrupt the fragile balance of mangrove ecosystems, affecting the health of plant and animal species that rely on them. Understanding pyridine's presence, sources, and effects in mangrove environments is crucial for conservation efforts and mitigating the impact of pollution on these biodiverse coastal ecosystems [45]. The microbial removal of pyridine from the environment is a promising strategy for the degradation [45].

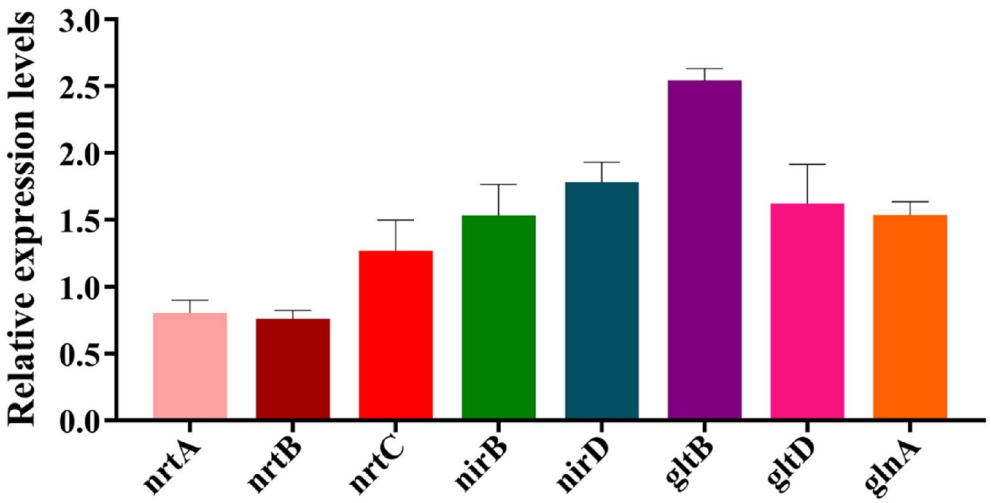

Fig. 6 Confirmation of gene expression of *nrtA*, *nrtB*, *nrtC*, *nirB*, *nirD*, *gltB*, *gltD*, and *glnA* genes through RT–qPCR analysis. The data are expressed as the mean ± SD

In this study, isolated *B. aryabhattai* strain NM1-A2, which can utilize pyridine as a carbon and nitrogen source, from subtropical marine mangrove sediments.

PH levels significantly impact the efficiency of xenobiotic degradation. Figure 1a illustrates a visual representation of different pH levels (ranging from 5.0 to 10.0) affect pyridine degradation in MSM. The optimal pyridine degradation was observed at an initial pH of 7.0, and complete pyridine degradation and maximum cell growth with a rate constant of 1.47×10^{-2}/h were achieved within 100 h. Our study is linked to the work of Shen et al., who found that NJUST18 showed expedited pyridine degradation at 126 and 122 h and at pH 5.0 and 10.0, respectively, with the initial pH of 9.0 [46]. Pyridine degradation and cell growth at the incubation temperatures of 35 °C and 40 °C were enhanced and substantially outperformed those at 25 °C and 30 °C with the rate constant of 1.76×10^{-2}/h. Kumar et al., reported a similar phenomenon when they enhanced the biodegradation of 4-*tert*-octylohenol and the proliferation of *Candida rugoo pelliculosa* RRKY5 at 30 °C [47].

The presence of exclusive biodegradable carbon sources often facilitates the degradation of persistent pollutants, such as pyridine. In the presence of 500 mg/L glucose, 500 mg/L pyridine could be eradicated. Adding 500 mg/L glucose also significantly enhanced cell growth. Increasing the supplemental glucose concentration to 1000, 1500, and 2000 mg/L significantly inhibited pyridine removal within 100 h and increased the rate constant to 2.91×10^{-2}/h. Shen et al. also illustrated that a low glucose dosage was beneficial for biomass production. In contrast, higher glucose consumption often led to competitive inhibition of pyridine biodegradation within a 140 h [46]. Our present investigation is consistent with the study of Mathur et al., who reported that *Shewanella putrefaciens* and *Bacillus sphaericus* could remove 500 mg/L pyridine after 140 and 150 h of incubation, respectively [28]. Li et al., discovered that *Streptomyces* sp. HJ02 could degrade 250 mg/L pyridine completely after 168 h [27]. Moreover, glucose can function as a carbon source for bacterial proliferation. On the other hand, pyridine, being a nitrogen-based aromatic compound, can also be employed as a carbon source for bacterial growth. Our study thoroughly investigated the effect of glucose concentration (0–2000 mg/L) on pyridine biodegradation to compare the growth of bacterial strains on refractory carbon-based pyridine and simple carbon sources, *i.e.*, glucose (nonaromatic). Our results demonstrated that 500 mg/L was the optimal concentration for the enhanced growth of NM1-A2. Within a 100 h incubation period, NM1-A2 exhibited substantial effectiveness as reflected by the apparent increase in its kinetics from 0.92×10^{-2}/h to 2.37×10^{-2}/h.

Liang et al., isolated NJUST18, NJUST29, and NJUST32 with mineralization performances of 41.54%, 56.89%, and 87.25%, respectively, based on their TOC removal efficiencies [33]. According to findings from other researchers, nitrogen in the pyridine ring is frequently converted into NH_4^+-N during pyridine biodegradation [39]. Past research has shown that *Paracoccus* is a good pyridine-degrading and denitrifying bacterium [48]. Additionally, our study also revealed that the nitrogen in the pyridine ring is typically converted into NH_4^+-N during pyridine biodegradation. Figure 3 shows that strain expansion resulted in a significant increase in NH_4^+-N. Specifically, the NH_4^+-N concentration increased to 55.31 ± 0.17 mg/L after 96 h. Additionally, Liu et al., discovered that TN concentration decreased from 369.00 ± 12.73 mg/L to 217.43 ± 10.51 mg/L at a removal rate of up to $40.51\%\pm1.21\%$, indicating a significant TN elimination [49]. In line with findings from a prior study [49], our research showed that approximately $51.3\%\pm2.39\%$ of total nitrogen (TN) was transformed into NH_4^+-N. NM1-A2 converts NO_2^- into NH_4^+ under anaerobic conditions [31]. Our study also aligned with a previous report showing that BW001 could grow by utilizing NO_3 and NO_2 converted from NH_3^- as nitrogen sources [31]. The concentration of the substrate is a crucial factor that impacts the rate of enzymatic reactions and has implications for bacterial growth as well as substrate degradation [49]. NH_4^+-N was formed during pyridine biodegradation by the strain and persisted in the environment [24, 50]. In a past work, 400 mg/L pyridine could not be degraded in a reactor even after 50 h of incubation with mixed activated sludge inoculated with *Pseudomonas pseudoalcaligenes*-KPN [51].

Our study performed three consecutive cycles of pyridine biodegradation. The performance of NM1-A2 was evaluated every 48 h for three cycles. After three successive cycles, pyridine degradation decreased by 4%. In alignment with previously reported results [39, 40], our finding demonstrated that NM1-A2 can be reused several times to degrade pyridine, a refractory nitrogen compound.

Nitrate or nitrite is transformed into ammonium inside cells for integration into carbon skeletons [52]. Nitrate is first converted into nitrite by NR; then, nitrite is converted into ammonium by NiR [53]. In our study, ammonium was primarily converted into glutamate through the glutamine synthetase (GS)/glutamate synthetase (GOGAT) cycle in nitrogen metabolism. In NM1-A2, the *Nrt-ABCD* nitrate transport family and *gltABCD* operons have been annotated. The *Nrt* family is accomplished for transporting extracellular nitrate, facilitating its transformation into intracellular NO_2 and NO_3. Within cells cultivated in

a glucose-ammonium medium, *gltC* was observed to promote *gltAB* transcription while also exerting a moderate repressive effect on *glnRA*, partially activating it. Ammonium ions (NH_4^+) have detrimental effects on plant cells, including the induction of proton extrusion, disruption of intracellular pH, and disentangling of photophosphorylation. As a result, it is advisable to rapidly assimilate NH_4^+ into non-toxic organic nitrogen molecules in order to prevent NH_4^+ toxicity [55]. The genes *nrtA*, *nrtB*, nrtC, and *nrtD* encode the proteins found in the *NrtABCD* transporter. Typically, they are part of the *nirA* operon, specifically in the order *nirA-nrtABCD-narB*, which is associated with the process of ammonium formation [56]. Tiffert et al., reported that cells grown in a glucose–ammonium medium required GS and glutamate synthetase activities and expressed the *glnRA* and *gltAB* operons at higher levels than cells grown in a glutamine medium [54]. Our study presented the NM1-A2, RT-qPCR validation analysis with reverence to all expressed genes (*nrtA*, *nrtB*, *nrtC*, *nirB*, *nirD*, *gltB*, *gltD*, *glnA*). Furthermore, NM1-A2 could be utilized to eliminate harmful ammonia byproducts, offering significant biotechnological and ecological potential.

Conclusion

The novel *B. aryabhattai* sp. strain NM1-A2 was isolated from mangrove sediments. Pyridine could be considered as the sole carbon and nitrogen source for its growth. In the presence of pyridine at varied concentrations of 100–2000 mg/L, the growth of the strain increased and the strain effectively degraded pyridine with high TOC removal efficacy. Notably, NM1-A2 released a substantial amount of NH_4^+, indicating that it has excellent pyridine biodegradation and NH_4^+ transformation efficiencies. The pseudo-first-order kinetics model was employed to describe the pyridine biodegradation pattern of NM1-A2. NM1-A2 showed fast pyridine degradation kinetics. The *nrt-ABCD* nitrate transport family and *gltABCD* operons found through KEGG annotation were involved in nitrogen metabolism. RT-qPCR analysis detected the nitrogen metabolism genes expression. This finding revealed that pyridine inhibits NM1-A2 enzymes. This research might be provided an avenue for using mangrove-based bacterial strains to treat refractory nitrogen compounds commercially.

Abbreviations

KEGG	Kyoto encyclopedia of genes and genomes
MEGA	Molecular evolutionary genetics analysis
GS	Glutamine synthetase
GOGAT	Glutamine 2-oxoglutarate aminotransferase
TOC	Total organic carbon
TN	Total nitrogen
NiR	Nitrite reductase
NR	Nitrate reductase

Supplementary Information

The online version contains supplementary material available at https://doi.org/10.1186/s40538-023-00513-5.

Additional file 1: Figure S1. Sample site collection and distribution are listed. Green labels R1, R2, and R3 indicate sampling sites in the rhizosphere area (rhizosphere roots within 3 cm). Red labels NR1, NR2, and NR3 indicate sampling sites in the non-rhizosphere area from near roots (rhizosphere roots within 1.5 m). While Yellow labels NM1, NM2, and NM3 (the rhizosphere and non-rhizosphere, within 100 m). **Figure S2.** Identification of nitrogen metabolism genes through gel electrophoresis. **Table S1.** All chemicals and medium. **Table S2.** Primers used in RT-qPCR.

Additional file 2: List of RT-qPCR gene sequences.

Acknowledgements

The author expresses their special gratitude to all the funding sources for the financial assistance and especially to Guangxi University.

Author contributions

CJ and LB: established the concept of the study. MK and SM: collected and processed samples. MK, LB, SM and YS: formed bioinformatics analyses. MK: wrote the draft. SK, SJS, MK, MH, TMK, JX, LB, JS, and CJ: revised and edited the manuscript. All authors have read and approved the manuscript's contents.

Funding

This research was supported by the Fund Project of Chinese Central Government Guiding to the Guangxi Local Science and Technology Development (Grant No. GUIKEZY21195021), the Natural Science Fund for Distinguished Young Scholars of Guangxi Zhuang Autonomous Region of China (Grant No. 2019GXNSFFA245011), the Funding Project of Chinese Central Government Guiding to the Nanning Local Science and Technology Development (Grant No. 20231012); the Funding Project of Technological Development from Angel Yeast (Chongzuo) Co., Ltd. (Grant No. JS1006020230722019), and the Basic Research Fund of Guangxi Academy of Sciences (Grant No. CQ-C-202202). The author expresses their special gratitude to all the funding sources for financial assistance, especially Guangxi University.

Availability of data and materials

The data described in this study can be obtained from the corresponding author upon request.

Declarations

Ethics approval and consent to participate

This manuscript is an original paper and has not been published in other journals. The authors agreed to keep the copyright rule.

Consent for publication

The author agreed to the publication of the manuscript in this journal.

Competing interests

The authors declare that they have no known competing financial interests or personal relationships that could have appeared to influence the work reported in this paper.

Author details
[1]National Engineering Research Center for Non-Food Biorefinery, State Key Laboratory of Non-Food Biomass and Enzyme Technology, Guangxi Research Center for Biological Science and Technology, Guangxi Academy of Sciences, Nanning 530007, China. [2]Guangxi Key Laboratory for Green Processing of Sugar Resources, College of Biological and Chemical Engineering, Guangxi University of Science and Technology, Liuzhou 545006, China. [3]Liuzhou Key Laboratory of Plant-Derived Ingredients of Liuzhou Luosifen, Liuzhou Special Food Flavor and Quality Control Research Center of Engineering Technology, Department of Food and Chemical Engineering, Liuzhou Institute of Technology, Liuzhou 545616, China. [4]Guangxi Key Laboratory of Beibu Gulf Marine Biodiversity Conservation, Beibu Gulf University, Qinzhou 535011, China. [5]State Key Laboratory for Conservation and Utilization of Subtropical Agro-Bioresources, Guangxi Research Center for Microbial and Enzyme Engineering Technology, College of Life Science and Technology, Guangxi University, Nanning 530004, China. [6]MOE Key Laboratory of New Processing Technology for Non-Ferrous Metals and Materials, Guangxi Key Laboratory of Processing for Non-Ferrous Metals and Featured Materials, School of Chemistry and Chemical Engineering, Guangxi University, Nanning 530004, China. [7]College of Resources and Environment, University of Chinese Academy of Sciences, 19 A Yuquan Road, Beijing 100049, China. [8]Research Center for Drug Discovery and Functional Food, Southwest Medical University, Luzhou, China.

Received: 15 August 2023 Accepted: 22 November 2023
Published online: 12 December 2023

References

1. Gil A, Taoufik N, García A, Korili SA. Comparative removal of emerging contaminants from aqueous solution by adsorption on an activated carbon. Environ Technol. 2018. https://doi.org/10.1080/09593330.2018.1464066.
2. Ma Q, Qu Y, Shen W, Zhang Z, Wang J, Liu Z, Li D, Li H, Zhou J. Bacterial community compositions of coking wastewater treatment plants in steel industry revealed by Illumina high-throughput sequencing. Biores Technol. 2015;179:436–43.
3. Zalat O, Elsayed M. A study on microwave removal of pyridine from wastewater. J Environ Chem Eng. 2013;1:137–43.
4. Majer B, Hofer E, Cavin C, Lhoste E, Uhl M, Glatt H, Meinl W, Knasmüller S. Coffee diterpenes prevent the genotoxic effects of 2-amino-1-methyl-6-phenylimidazo [4, 5-b] pyridine (PhIP) and N-nitrosodimethylamine in a human derived liver cell line (HepG2). Food Chem Toxicol. 2005;43:433–41.
5. Saroha AK. Biodegradability enhancement of industrial organic raffinate containing pyridine and its derivatives by CWAO using ceria promoted MnOx/Al2O3 catalyst at atmospheric pressure. Chem Eng J. 2018;334:985–94.
6. Bouyarmane H, El Asri S, Rami A, Roux C, Mahly M, Saoiabi A, Coradin T, Laghzizil A. Pyridine and phenol removal using natural and synthetic apatites as low cost sorbents: influence of porosity and surface interactions. J Hazard Mater. 2010;181:736–41.
7. Li Y, Yi R, Yi C, Zhou B, Wang H. Research on the degradation mechanism of pyridine in drinking water by dielectric barrier discharge. J Environ Sci. 2017;53:238–47.
8. Bai Y, Sun Q, Zhao C, Wen D, Tang X. Aerobic degradation of pyridine by a new bacterial strain, Shinella zoogloeoides BC026. J Ind Microbiol Biotechnol. 2009;36:1391–400.
9. Rajput MS, Dwivedi V, Awasthi S. Biodegradation of pyridine raffinate by microbial laccase isolated from Pseudomonas monteilii & Gamma proteobacterium present in woody soil. Biocatal Agric Biotechnol. 2020;26:101650.
10. Bai Y, Sun Q, Xing R, Wen D, Tang X. Removal of pyridine and quinoline by bio-zeolite composed of mixed degrading bacteria and modified zeolite. J Hazard Mater. 2010;181:916–22.
11. SI Mulla, F Ameen, MP Talwar, SAMAS Eqani, RN Bharagava, G Saxena, PN Tallur, HZ Ninnekar. Organophosphate pesticides: impact on environment, toxicity, and their degradation, bioremediation of industrial waste for environmental safety: Volume I: industrial waste and its management. 2020. 265–290.
12. Sun J-Q, Xu L, Tang Y-Q, Chen F-M, Liu W-Q, Wu X-L. Degradation of pyridine by one Rhodococcus strain in the presence of chromium (VI) or phenol. J Hazard Mater. 2011;191:62–8.
13. Mattocks S, Hall CJ, Jordaan A. Damming, lost connectivity, and the historical role of anadromous fish in freshwater ecosystem dynamics. Bioscience. 2017;67:713–28.
14. Aranda M, Peralta G, Montes J, Gracia F, Fivash G, Bouma T, van der Wal D. Salt marsh fragmentation in a mesotidal estuary: Implications for medium to long-term management. Sci Total Environ. 2022;846:157410.
15. Giri C, Ochieng E, Tieszen LL, Zhu Z, Singh A, Loveland T, Masek J, Duke N. Status and distribution of mangrove forests of the world using earth observation satellite data. Glob Ecol Biogeogr. 2011;20:154–9.
16. Nie Z, Yan B, Xu Y, Awasthi MK, Yang H. Characterization of pyridine biodegradation by two Enterobacter sp. strains immobilized on Solidago canadensis L. stem derived biochar. J Hazardous Mater. 2021;414:125577.
17. Huarancca Reyes T, Scartazza A, Pompeiano A, Ciurli A, Lu Y, Guglielminetti L, Yamaguchi J. Nitrate reductase modulation in response to changes in C/N balance and nitrogen source in Arabidopsis. Plant Cell Physiol. 2018;59:1248–54.
18. Hossain M, Uddin M, Ismail MR, Ashrafuzzaman M. Responses of glutamine synthetase-glutamate synthase cycle enzymes in tomato leaves under salinity stress. Int J Agric Biol. 2012;14(4):509.
19. de Souza Miranda R, Gomes-Filho E, Prisco JT, Alvarez-Pizarro JC. Ammonium improves tolerance to salinity stress in Sorghum bicolor plants. Plant Growth Regul. 2016;78:121–31.
20. Lin Z, Pang S, Zhou Z, Wu X, Li J, Huang Y, Zhang W, Lei Q, Bhatt P, Mishra S. Novel pathway of acephate degradation by the microbial consortium ZQ01 and its potential for environmental bioremediation. J Hazard Mater. 2022;426:127841.
21. Zan Z-Y, Ge X-F, Huang R-R, Liu W-Z. Pseudonocardia humida sp. nov., an actinomycete isolated from mangrove soil showing distinct distribution pattern of biosynthetic gene clusters. Current Microbiol. 2022;79:87.
22. Takagi K, Iwasaki A, Kamei I, Satsuma K, Yoshioka Y, Harada N. Aerobic mineralization of hexachlorobenzene by newly isolated pentachloronitrobenzene-degrading Nocardioides sp. strain PD653. Appl Environ Microbiol. 2009;75:4452–8.
23. Wang J, Jiang X, Liu X, Sun X, Han W, Li J, Wang L, Shen J. Microbial degradation mechanism of pyridine by Paracoccus sp. NJUST30 newly isolated from aerobic granules. Chem Eng J. 2018;344:86–94.
24. Lin Q, Donghui W, Jianlong W. Biodegradation of pyridine by Paracoccus sp. KT-5 immobilized on bamboo-based activated carbon. Bioresour Technol. 2010;101:5229–34.
25. Berg KA, Lyra C, Sivonen K, Paulin L, Suomalainen S, Tuomi P, Rapala J. High diversity of cultivable heterotrophic bacteria in association with cyanobacterial water blooms. ISME J. 2009;3:314–25.
26. Chandra R, Bharagava RN, Kapley A, Purohit HJ. Isolation and characterization of potential aerobic bacteria capable for pyridine degradation in presence of picoline, phenol and formaldehyde as co-pollutants. World J Microbiol Biotechnol. 2009;25:2113–9.
27. Li J, Cai W, Cai J. The characteristics and mechanisms of pyridine biodegradation by Streptomyces sp. J Hazard Mater. 2009;165:950–4.
28. Mathur AK, Majumder C, Chatterjee S, Roy P. Biodegradation of pyridine by the new bacterial isolates S. putrefaciens and B. sphaericus. J Hazardous Mater. 2008;157:335–43.
29. Kashif M, Sang Y, Mo S, Ur Rehman S, Khan S, Khan MR, He S, Jiang C. Deciphering the biodesulfurization pathway employing marine mangrove Bacillus aryabhattai strain NM1-A2 according to whole genome sequencing and transcriptome analyses. Genomics. 2023;115:110635.
30. Shen J, He R, Wang L, Zhang J, Zuo Y, Li Y, Sun X, Li J, Han W. Biodegradation kinetics of picric acid by Rhodococcus sp. NJUST16 in batch reactors. J Hazardous Mater. 2009;167:193–8.
31. Bai Y, Sun Q, Zhao C, Wen D, Tang X. Microbial degradation and metabolic pathway of pyridine by a Paracoccus sp. strain BW001. Biodegradation. 2008;19:915–26.
32. Callaghan MM, Dillard JP. Transformation in Neisseria gonorrhoeae. Neisseria Gonorrhoeae Methods Protocols. 2019. https://doi.org/10.1007/978-1-4939-9496-0_10.
33. Liang J, Li W, Zhang H, Jiang X, Wang L, Liu X, Shen J. Coaggregation mechanism of pyridine-degrading strains for the acceleration of the aerobic granulation process. Chem Eng J. 2018;338:176–83.

34. Frontistis IT. Photocatalytic and photoelectrocatalytic degradation of. Chemosphere. 2006;63:1087–93.
35. Datta A, Philip L, Bhallamudi SM. Modeling the biodegradation kinetics of aromatic and aliphatic volatile pollutant mixture in liquid phase. Chem Eng J. 2014;241:288–300.
36. Feng H, Wang Y, Zhang X, Shen D, Li N, Chen W, Huang B, Liang Y, Zhou Y. Degradation of p-fluoronitrobenzene in biological and bioelectrochemical systems: differences in kinetics, pathways, and microbial community evolutions. Chem Eng J. 2017;314:232–9.
37. Zhou L, Boyd CE. Comparison of Nessler, phenate, salicylate and ion selective electrode procedures for determination of total ammonia nitrogen in aquaculture. Aquaculture. 2016;450:187–93.
38. Liu Y, Zhang Q, Lv Y, Ren R. Pyridine degradation characteristics of a newly isolated bacterial strain and its application with a novel reactor for the further treatment in pyridine wastewater. Process Biochem. 2020;95:64–70.
39. Qiao L, Wang J-L. Microbial degradation of pyridine by Paracoccus sp. isolated from contaminated soil. J Hazardous Mater. 2010;176:220–5.
40. Huang D, Liu W, Wu Z, Liu G, Yin H, Chen Y, Hu N, Jia L. Removal of pyridine from its wastewater by using a novel foam fractionation column. Chem Eng J. 2017;321:151–8.
41. Rütting T, Boeckx P, Müller C, Klemedtsson L. Assessment of the importance of dissimilatory nitrate reduction to ammonium for the terrestrial nitrogen cycle. Biogeosciences. 2011;8:1779–91.
42. Scanlan DJ, Ostrowski M, Mazard S, Dufresne A, Garczarek L, Hess WR, Post AF, Hagemann M, Paulsen I, Partensky F. Ecological genomics of marine picocyanobacteria. Microbiol Mol Biol Rev. 2009;73:249–99.
43. Yang Y, Xu X, Jing Z, Ye J, Li H, Li X, Shi L, Chen M, Wang T, Xie B. Genome-wide screening and stability verification of the robust internal control genes for RT-qPCR in filamentous fungi. Journal of Fungi. 2022;8:952.
44. Mazur D, Detenchuk E, Sosnova A, Artaev V, Lebedev A. GC-HRMS with complementary ionization techniques for target and non-target screening for chemical exposure: expanding the insights of the air pollution markers in Moscow snow. Sci Total Environ. 2021;761:144506.
45. Tian F, Zhu R, Ouyang F. Synergistic photocatalytic degradation of pyridine using precious metal supported TiO2 with KBr O3. J Environ Sci. 2013;25:2299–305.
46. Shen J, Chen Y, Wu S, Wu H, Liu X, Sun X, Li J, Wang L. Enhanced pyridine biodegradation under anoxic condition: the key role of nitrate as the electron acceptor. Chem Eng J. 2015;277:140–9.
47. Kumar Rajendran R, Huang S-L, Lin C-C, Kirschner R. Biodegradation of the endocrine disrupter 4-tert-octylphenol by the yeast strain Candida rugopelliculosa RRKY5 via phenolic ring hydroxylation and alkyl chain oxidation pathways. Bioresour Technol. 2017;226:55–64.
48. Yang X, Ye J, Lyu L, Wu Q, Zhang R. Anaerobic biodegradation of pyrene by Paracoccus denitrificans under various nitrate/nitrite-reducing conditions. Water Air Soil Pollut. 2013;224:1–10.
49. Liu X, Wu S, Zhang D, Shen J, Han W, Sun X, Li J, Wang L. Simultaneous pyridine biodegradation and nitrogen removal in an aerobic granular system. J Environ Sci. 2018;67:318–29.
50. Xu P, Wei Y, Cheng N, Li S, Li W, Guo T, Wang X. Evaluation on the removal performance of dichloromethane and toluene from waste gases using an airlift packing reactor. J Hazard Mater. 2019;366:105–13.
51. Padoley K, Rajvaidya A, Subbarao T, Pandey R. Biodegradation of pyridine in a completely mixed activated sludge process. Biores Technol. 2006;97:1225–36.
52. Stripp ST, Duffus BR, Fourmond V, Léger C, Leimkühler S, Hirota S, Hu Y, Jasniewski A, Ogata H, Ribbe MW. Second and outer coordination sphere effects in nitrogenase, hydrogenase, formate dehydrogenase, and CO dehydrogenase. Chem Rev. 2022;122:11900–73.
53. Oliver NJ, Rabinovitch-Deere CA, Carroll AL, Nozzi NE, Case AE, Atsumi S. Cyanobacterial metabolic engineering for biofuel and chemical production. Curr Opin Chem Biol. 2016;35:43–50.
54. Tiffert Y, Supra P, Wurm R, Wohlleben W, Wagner R, Reuther J. The Streptomyces coelicolor GlnR regulon: identification of new GlnR targets and evidence for a central role of GlnR in nitrogen metabolism in actinomycetes. Mol Microbiol. 2008;67:861–80.
55. Zhang Y, Zhang L, Hu X-H. Exogenous spermidine-induced changes at physiological and biochemical parameters levels in tomato seedling grown in saline-alkaline condition. Bot Stud. 2014;55:1–8.
56. Patel A, Tiwari S, Prasad SM. Effect of time interval on arsenic toxicity to paddy field cyanobacteria as evident by nitrogen metabolism, biochemical constituent, and exopolysaccharide content. Biol Trace Elem Res. 2021;199:2031–46.

Publisher's Note